Theoretical calculating the thermodynamic properties of solid sorbents for CO_2 capture applications

Yuhua Duan[1]
National Energy Technology Laboratory, United States Department of Energy,
Pittsburgh, Pennsylvania 15236, USA

Abstract

Since current technologies for capturing CO_2 to fight global climate change are still too energy intensive, there is a critical need for development of new materials that can capture CO_2 reversibly with acceptable energy costs. Accordingly, solid sorbents have been proposed to be used for CO_2 capture applications through a reversible chemical transformation. By combining thermodynamic database mining with first principles density functional theory and phonon lattice dynamics calculations, a theoretical screening methodology to identify the most promising CO_2 sorbent candidates from the vast array of possible solid materials has been proposed and validated. The calculated thermodynamic properties of different classes of solid materials versus temperature and pressure changes were further used to evaluate the equilibrium properties for the CO_2 adsorption/desorption cycles. According to the requirements imposed by the pre- and post- combustion technologies and based on our calculated thermodynamic properties for the CO_2 capture reactions by the solids of interest, we were able to screen only those solid materials for which lower capture energy costs are expected at the desired pressure and temperature conditions. Only those selected CO_2 sorbent candidates were further considered for experimental validations. The *ab initio* thermodynamic technique has the advantage of identifying thermodynamic properties of CO_2 capture reactions without any experimental input beyond crystallographic structural information of the solid phases involved. Such methodology not only can be used to search for good candidates from existing database of solid materials, but also can provide some guidelines for synthesis new materials. In this presentation, we first introduce our screening methodology and the results on a testing set of solids with known thermodynamic properties to validate our methodology. Then, by applying our computational method to several different kinds of solid systems, we demonstrate that our methodology can predict the useful information to help developing CO_2 capture Technologies.

I. Introduction

Carbon dioxide is one of the major combustion products which once released into the air can contribute to the global climate warming effects.[1-3] In order to mitigate the global climate change, CO_2 emissions into the atmosphere must be stopped by separating and capturing CO_2 from coal combustion and gasification plants and sequestering the CO_2 underground. Figure 1 shows a schematic of CO_2 capture, storage and utilization. Among them, CO_2 capture is economically the key step and has three technology routes: (1) post-combustion: capture CO_2 from the flue gas

[1] Author to whom correspondence should be addressed. Tel. 412-386-5771, Fax 412-386-5920, E-mail: yuhua.duan@netl.doe.gov

stream after combustion; (2) pre-combustion: capture from the reformed synthesis gas of an upstream gasification unit; (3) oxyfuel: first separation the oxygen from the air and then use of the nearly pure oxygen for fuel combustion to obtain pure CO_2. Captured CO_2 will be largely sequestered underground. As shown in Figure1, the captured CO_2 also could be used for enhancing oil recovery as well as carbon resources to be converted into other useful compounds[4-6].

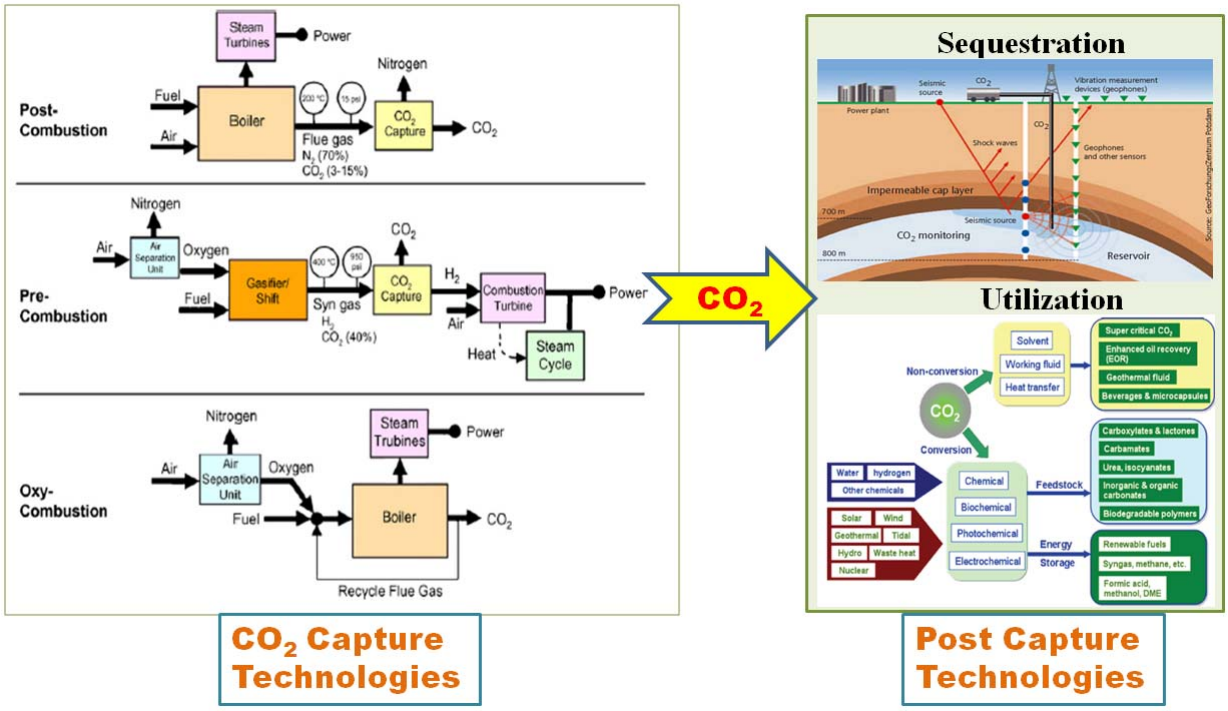

Figure 1. Schematic representation of CO_2 production, capture, storage and utilization[7].

During the past few decades, many efforts have been devoted to new technologies for CO_2 capture, sequestration and utilization.[4-6,8] Current technologies for capturing CO_2 including solvent-based (amines) and CaO-based materials are still too energy intensive. Hence, there is critical need for new materials that can capture and release CO_2 reversibly with acceptable energy costs. Accordingly, solid sorbent materials have been proposed for capturing CO_2 through a reversible chemical transformation and most of them result in the formation of carbonate products. Solid sorbents containing alkali and alkaline earth metals have been reported in several previous studies to be good candidates for CO_2 sorbent applications due to their high CO_2 absorption capacity at moderate working temperatures.[9-11]

To achieve such goals, one of these new methods considered at National Energy Technology Laboratory (NETL) is based on the use of regenerable solid sorbents. In this case sorbents such as alkaline earth metal oxides or hydroxides are used to absorb CO_2 at warm temperatures typically ranging from ~100-300 °C.[12-13] The key phenomenon in these processes is transformation of the oxide or hydroxide materials to a carbonate upon CO_2 absorption. Regeneration of the sorbent can be obtained, if necessary, in a subsequent step represented by the reverse transformation from the carbonate phase to the oxide or hydroxide phases either through temperature swing or through pressure swing. The efficiencies of these processes are highly dependent on identification of the optimum temperature and pressure conditions at which the absorption, and regeneration are performed. In the case of high-performance sorbents, both these two mechanistic steps are optimized in order to achieve minimal energetic and operational costs.

Optimization of the sorbent material can be obtained starting from the analysis of its intrinsic atomistic structure and of transformations upon interaction with CO_2. Of particular importance is to identify the corresponding thermodynamic and kinetic characteristics of the sorbent material of interest. For this purpose scientists at NETL have developed a multi-step computational methodology based on combined use of first principles calculations combined with lattice phonon dynamics to describe the thermodynamic properties of CO_2 capture reactions by solid sorbents.[9,14-20] This methodology has been used to screen different classes of solid compounds and has, as a major objective, identification of the optimum candidate materials that can be further subjected to experimental testing. The advantage of this proposed method is that it allows identification of the thermodynamic properties of the CO_2 capture reaction as a function of temperature and pressure without any experimental input, except for the crystallographic structural information of the solid phases involved. Such thermodynamic information is essential to guide experimental groups at NETL in development of highly optimized CO_2 sorbents. For a given database of solid materials, our screening scheme allows identification of a short list of promising candidates of CO_2 sorbents with optimal energy usages, which can be further evaluated by our experimental research groups.

In this presentation, we summarize our progress on the development of novel screening scheme to indentify most promising candidates for CO_2 sorbents which could be used for either post-combustion or in pre-combustion CO_2 capture technology. The remainder of this report is organized as follows: In the second section we briefly describe the screening method we developed. In the third section, we first provide the validation results of our computational method for the case of alkali and alkaline metal compounds. Then, we present some preliminary results on CO_2 capture reactions by lithium related silicate and zirconate compounds. The main conclusions are summarized in the last section.

II. Screening Methodology

2.1 *ab initio* thermodynamics approach

The complete description of the computational methodology can be found in our previous papers.[9,14-23] Here, we limit ourselves to provide only the main aspects relevant for the current study. The CO_2 capture reactions by solids in the presence of water vapor can be expressed generically in the form

$$\text{Solid\_A} + n_1 CO_2 \leftrightarrow \text{Solid\_B} + [\text{Solid\_C}] \pm n_2 [H_2O] \qquad (1)$$

where the terms given in […] are optional and n_1 and n_2 are the numbers of moles of CO_2 and H_2O involved in the capture reactions. We treat the gas phase species CO_2 and H_2O as ideal gases. By assuming that the difference between the chemical potentials ($\Delta\mu^o$) of the solid phases of A, B (and C) can be approximated by the difference in their electronic energies (ΔE^o), obtained directly from first-principles DFT calculations, and the vibrational free energy of the phonons and by ignoring the PV contribution terms for solids, the variation of the chemical potential ($\Delta\mu$) for capture reaction with temperature and pressure can be written as

$$\Delta\mu(T,P) = \Delta\mu^0(T) - RT \ln \frac{P_{CO_2}^{n_1}}{P_{H_2O}^{\pm n_2}} \qquad (2)$$

where $\Delta\mu^0(T)$ is the standard chemical potential changes between reactants and products. If these thermodynamical data are available in the thermodynamic database or literature, we can direct

apply them into above equation. If these data are not available, they can be calculated using the *ab initio* thermodynamic approach based on the following approximation.

$$\Delta\mu^0(T) \approx \Delta E^{DFT} + \Delta E_{ZP} + \Delta F^{PH}(T) - n_1 G_{CO_2}(T) \pm n_2 G_{H_2O}(T) \quad (3)$$

Here, ΔE_{ZP} is the zero point energy difference between the reactants and products and can be obtained directly from phonon calculations. The ΔF^{PH} is the phonon free energy change between the solids of products and reactants. If the capture reaction does not involve H_2O, then the P_{H_2O} in above equations is set to P_0, which is the standard state reference pressure of 1 bar, and the G_{H_2O} term is not present. The "+" and "-" signs correspond to the cases when H_2O is a product, respectively a reactant, in the general reaction. The free energies of CO_2 (G_{CO_2}) and H_2O (G_{H_2O}) can be obtained from standard statistical mechanics. The enthalpy change for the reaction (1), $\Delta H^{cal}(T)$, can be derived from above equations as

$$\Delta H^{cal}(T) = \Delta\mu^0(T) + T(\Delta S_{PH}(T) - n_1 S_{CO_2}(T) \pm n_2 S_{H_2O}) \quad (4)$$

In Eq.(3), ΔE^{DFT} is the total energy change of the reactants and products calculated by DFT. In this work, the Vienna *Ab-initio* Simulation Package (VASP)[24-25] was employed to calculate the electronic structures of the solid materials involved in this study. All calculations have been done using the projector augmented wave (PAW) pseudo-potentials and the PW91 exchange-correlation functional.[26] This computational level was shown to provide an accurate description of oxide systems.[18-19,27] Plane wave basis sets were used with a cutoff energy of 500 eV and a kinetic energy cutoff for augmentation charges of 605.4 eV. The k-point sampling grids of $n_1 \times n_2 \times n_3$, obtained using the Monkhorst-Pack method,[28] were used for these bulk calculations, where n_1, n_2, and n_3 were determined consistent to a spacing of about 0.028 $Å^{-1}$ along the axes of the reciprocal unit cells. In Eqs.(3) and (4), the zero-point-energies(E_{ZP}), entropies (S_{PH}), and harmonic free energies (F^{PH}, excluding zero-point energy which was already counted into the term ΔE_{ZP}) of solids were calculated by the PHONON software package[29] in which the direct method is applied following the formula derived by Parlinski *et al.*[30] to combine *ab initio* DFT with lattice phonon dynamics calculations.

Based on phonon calculations under the harmonic approximation, the phonon free energy ΔF^{PH} change between reactant and product solids can be calculated through the free energy of solids described by the Helmholtz form F_{harm} as shown in Eq.(2) and the entropy of the solids (S_{harm})

$$\Delta F^{PH}(T) = \Delta F_{harm}(T) - T\Delta S_{harm}(T) \quad (5)$$

where the F_{harm}, S_{harm} and the internal energy(E_{tot}) of the solids are defined as [31]

$$F_{harm}(T) = rk_B T\int_0^\infty g(\omega)\ln[2\sinh(\frac{\hbar\omega}{2k_B T})]d\omega \quad (6)$$

$$S_{harm}(T) = rk_B\int_0^\infty g(\omega)\{(\hbar\frac{\hbar\omega}{2k_B T})[\coth(\frac{\hbar\omega}{2k_B T}) - 1] - \ln[1 - \exp(-\frac{\hbar\omega}{k_B T}]\}d\omega \quad (7)$$

$$E_{tot}(T) = \frac{1}{2}r\int_0^\infty g(\omega)(\hbar\omega)\coth(\frac{\hbar\omega}{2k_B T})d\omega \quad (8)$$

where r is the number of degree of freedom in the primitive unit cell. It can be seen that the zero-point-energy (E_{ZP}) can be obtained from Eq.(5) by taking $T \to 0$.

$$E_{ZP} = \lim_{T\to 0}(E_{tot}(T)) \quad (9)$$

where ω is the phonon dispersion frequency, and g(ω) is the phonon density of state. In this study, we employed the PHONON software package[29] in which the direct method is applied following the formalism derived by Parlinski *et al.*[30] In phonon calculations, a supercell was created from the optimized unit cell structure that was calculated based on DFT. Structures with a displacement of 0.03Å of non-equivalent atoms were generated from the supercell and DFT calculations were further performed to obtain the force on each atom due to the displacements. These forces were input into the PHONON package[29] to fit the force matrix and further carry out the phonon dispersions and densities, which can be inputted into Eqs.(6)-(8) to calculate the thermodynamic properties.

As an optimal CO_2 solid sorbent, it should not only be easy to absorb CO_2 in the capture cycle but also be easy to release the CO_2 during regeneration cycle. The operating conditions for absorption/desorption processes depend on the sorbent use as in a pre- or a post-combustion application. The US Department of Energy (DOE) programmatic goal for post-combustion and oxy-combustion CO_2 capture is to capture at least 90% of the CO_2 produced by a plant with the cost in electricity increasing no more than 35%, whereas the goal in the case of pre-combustion CO_2 capture is to capture at least 90% of the CO_2 produced with the cost in electricity increasing no more than 10%.[7,32-33] Under pre-combustion conditions, after the water-gas shift reactor, the gas stream mainly contains CO_2, H_2O and H_2. The partial CO_2 pressure could be as high as 20 to 30 bar and the temperature (T_1) is around 313~573K. To minimize the energy consumption, the ideal sorbents should work in these ranges of pressure and temperature in order to separate CO_2 from H_2. For post-combustion conditions, the gas stream mainly contains CO_2 H_2O, and N_2, the partial pressure of CO_2 is in the range 0.1 to 0.2 bar, and the temperature (T_2) range is quite different. Currently, in post-combustion CO_2 capture technology, amine-based solvents, carbon- and zeolite-based solid sorbents (including metal organic framework) capture CO_2 within a lower temperature range (<200°C),[34] while oxides (such as CaO, Na_2O, *etc*.) and salts (such as Li_4SiO_4, Li_2ZrO_3, *etc*) capture CO_2 usually within a higher temperature range (>400°C).[14-18] Based on Eq.(2), the working conditions of each solid capturing CO_2 can be evaluated and used for determining its suitability as CO_2 sorbent.

In this study, the thermodynamic database HSC Chemistry[35] and Factsage[36] packages were employed to search for the available thermodynamic properties of solids.

2.2 Screening scheme

Figure 2 shows the schematic of our screening methodology. For a given solid databank, this methodology includes four main screening steps (or filters) which allow identification of the most promising candidates:[18,21]

Step 1: For each solid in the data bank, we first conduct basic screening based on acquisition of general data, such as the weight percent (wt%) of absorbed CO_2 in the assumption of a complete reaction, the materials safety and cost, *etc.* We also include, where available, the thermodynamic data from literature and from general thermodynamic databases, such as HSC Chemistry, Factsage, *etc*. If the necessary data for evaluation of the thermodynamic properties exists, then the use of DFT calculations is not necessary and the optimal candidates can be obtained by minimizing their known free energies based on the operating conditions. Otherwise, if the material passes basic screening, but no thermodynamic data are available, then we continue to the next step.

Step 2: Perform DFT calculations for all compounds in the candidate reaction with this solid. If $|\Delta E^{DFT} - \Delta E_{ref}|/n_1 < 20$ kJ/mol, where n_1 is CO_2 molar number in capture reaction, and ΔE_{ref} is the DFT energy change for the reference capture reaction (*e.g.* $CaO+CO_2=CaCO_3$), we add this compound to the list of good candidates. Otherwise, we go back to *step 1* and pick another solid.

Step 3: Perform phonon calculations for reactant and product solids to obtain the corresponding zero point energies and the phonon free energies for the list of good candidates.

Specify the target operating conditions (temperature, partial pressures of CO_2 and H_2O) and compute the change in chemical potential for the reaction, namely $\Delta\mu(T, P)$ from above equations. If $\Delta\mu(T, P)$ is close to zero (*e.g.* $|\Delta\mu(T, P)| < 5$ kJ/mol) at the operating conditions, then we select this reaction as a member of the "better" list. Only a short list of compounds will likely be left after application of *step 3*.

Step 4: Additional modeling could be performed to rank the remaining short list of better candidates both obtained from database searching and *ab initio* thermodynamic calculations as shown in figure 1. One is the kinetics of the capture reactions, which could be done by transport and diffusion calculations as well as using experimental measurements. Another necessary and doable modeling task is the behavior of the solid in the reactor, which can be done by computational fluid dynamics (CFD) methods based on finite element method (FEM) approach and process modeling to estimate the overall costs.[37] These simulations are currently underway. Application of these screening filters will ensure that only the most promising candidates will be identified for the final experimental testing.

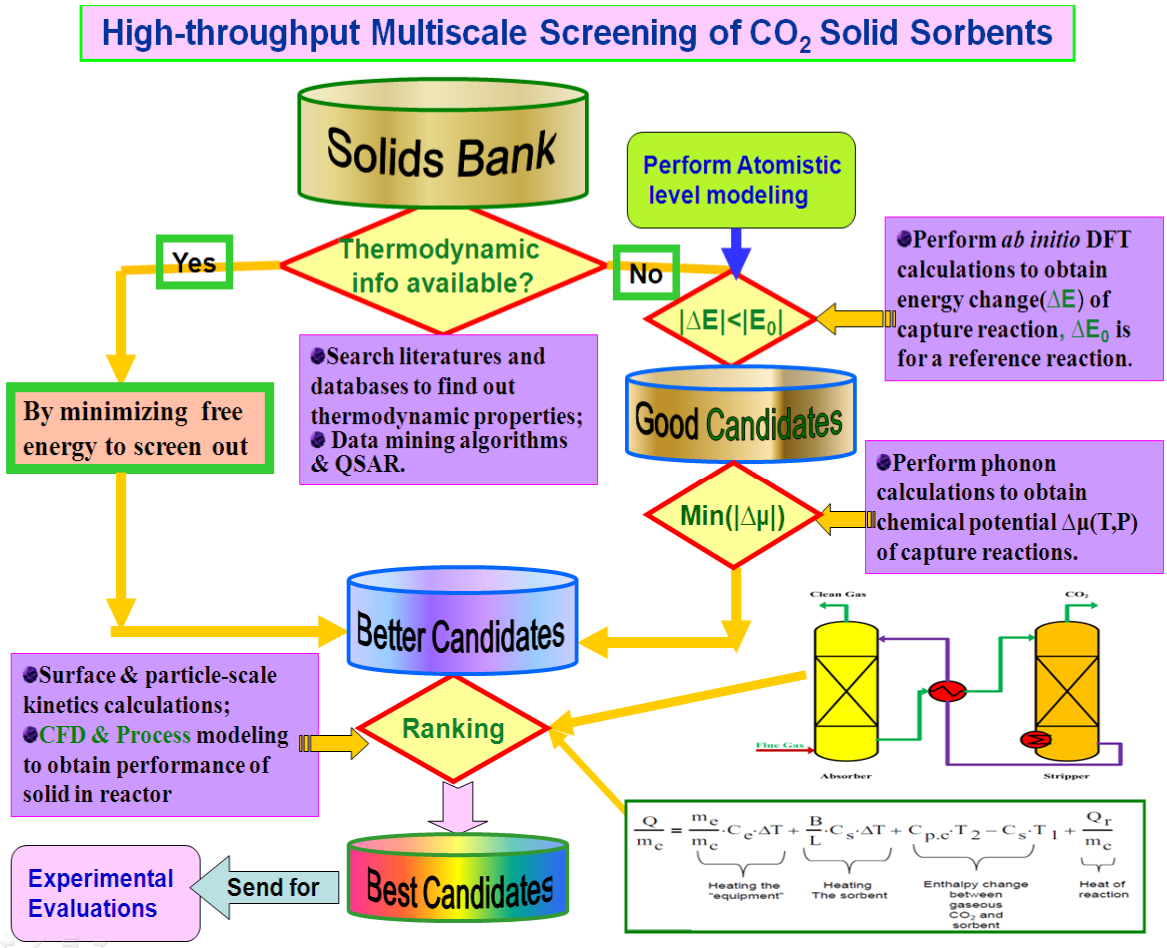

Figure 2. Schematic of our screening methodology

This screening methodology provides a path for evaluating materials for which experimental thermodynamic data are unavailable. One area where this approach could be used to great advantage is in evaluating mixtures and doped materials, where thermodynamic data are generally not available but for which the crystallographic structure is known or can be easily determined. Based on the above screening methodology, we have screened hundreds of solid compounds and

found some promising candidates for CO_2 sorbents. Here, in this work we summarize the results obtained by applying the screening methodology to several classes of solid materials.

III. Results and Discussions

3.1 Applications to alkali and alkaline earth metal oxides and hydroxides[9,17-20]

The thermodynamic data for the alkali and alkaline earth metal oxides, hydroxides and corresponding carbonates and bicarbonates are available in thermodynamic databases[35-36]. In order to validate our theoretical approach, we also made the *ab initio* thermodynamic calculations for these known crystals.

As an example, Figure 3 shows the calculated and experimental measured thermodynamic properties of the reactions for alkali and alkaline earth metal oxides capture of CO_2. From it, one can see that, except for $BeO+CO_2 \rightarrow BeCO_3$ reaction, overall, the calculated results are in good agreement with HSC experimental data. These findings indicate that our theoretical approach can predict the right thermodynamic properties of various solid reacting with CO_2 if the right crystal structure is known or is easy to be determined. The larger discrepancy observed for $BeO/BeCO_3$ system is due to lack of the crystal structure information of $BeCO_3$. As the only one input property of the solid in the *ab initio* thermodynamics calculations, this indicates that in order to obtain reliable results, the crystal structure must be known or can be easily predicted correctly.

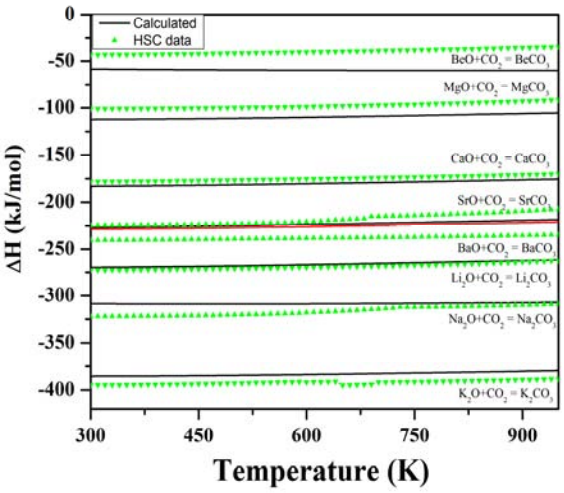

(a)

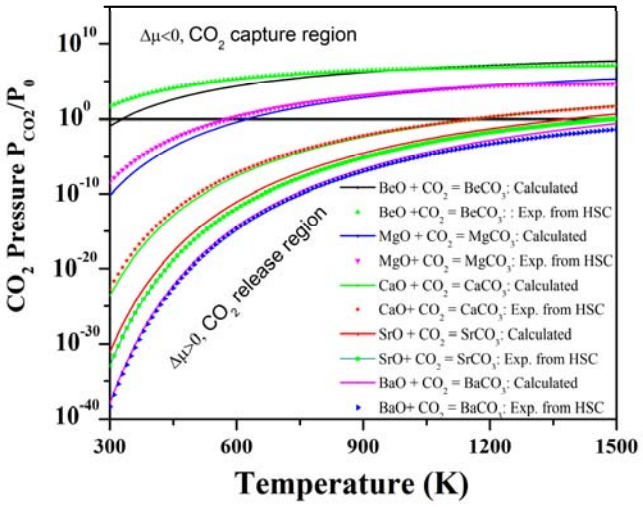

(b)

Figure 3. (a) The calculated heats of reaction as a function of temperature for eight metal oxides. The solid lines were computed from DFT including phonon contributions. The dashed lines were computed from the HSC package. The discontinuities in the HSC curves indicate phase transitions; (b) The calculated chemical potentials (Gibbs free energy) versus CO_2 pressures (in logarithm scale) and temperatures for the reactions of oxides capturing CO_2 without water involved.

As summarized in Fig.4, among the 24 CO_2 capture reactions of these solids, after applying the first filter (steps 1 & 2), only 10 reactions satisfied our selection criteria and are worth consideration for the third screening step (filter two). After applying the second filter on these 10 reactions, as shown in Fig. 4, we found that only $MgO/Mg(OH)_2$, $Na_2CO_3/NaHCO_3$, $K_2CO_3/KHCO_3$ are promising candidates for CO_2 sorbents in either post-combustion or pre-

combustion CO_2 capture technologies.[7,8,10] These results are in good agreement with the experimental facts, which means our screening methodology is reliable and could be used to identify promising solid CO_2 sorbents by predicting the thermodynamic properties of solids reacting with CO_2.[19]

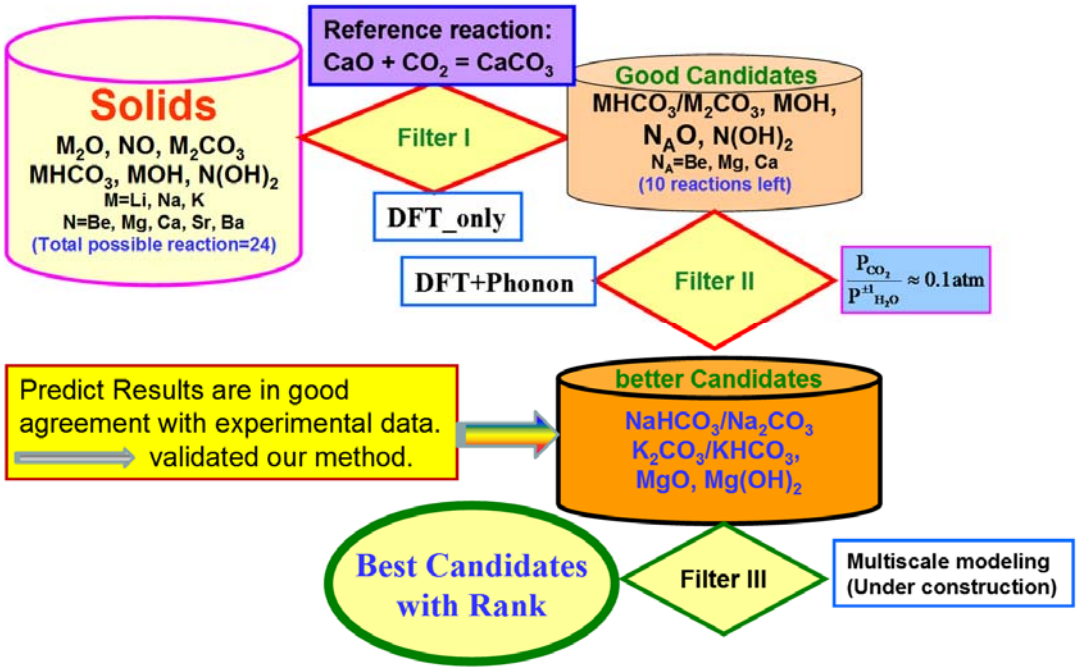

Figure 4. Schematic screening results of alkali and alkaline metal oxides, hydroxides and bicarbonates.

Based on Eq.(2), Fig. 5 gives the calculated relationships of the chemical potential $\Delta\mu(T,P)$ with temperature and CO_2 pressure for reactions $M_2CO_3+CO_2+H_2O = 2MHCO_3$ (M=Na, K), $MgO + CO_2 = MgCO_3$, and $Mg(OH)_2 + CO_2 = MgCO_3 + H_2O$. From Fig. 5, one can see that $Na_2CO_3/NaHCO_3$ and $K_2CO_3/KHCO_3$ can capture CO_2 at low temperature range (400~500K) when CO_2 pressure is around 0.1bar (post-combustion) or 20~30 bar (pre-combustion).[15,19] We have examined the effect of H_2O on the reaction thermodynamics and have found that our modeling approach can be used to account for partial pressures of CO_2 and H_2O and the temperature. We found that formation of bicarbonates from the alkali metal oxides results in a lower sorbent regeneration temperature and that formation of bicarbonate from the carbonates, by addition of CO_2 and H_2O, reduces the CO_2 capturing temperature even further. Indeed, as shown in Fig.4, we predict that Na_2CO_3 and K_2CO_3 have turnover temperatures for CO_2 capture through bicarbonate formation that are suitable for operation under both pre- and post-combustion conditions. When the steam pressure (P_{H_2O}) increases as shown in Fig.5, at the same temperature, the P_{CO_2} is decreased because both CO_2 and H_2O are on the reactant sides.

As one can see from Fig.5, our results show that MgO could be used for both pre- and post-combustion capture technologies due to its low regenerating temperature (T_2=540 K for post-combustion conditions and T_1=690 K for pre-combustion conditions) which are close to experimental findings. However, $Mg(OH)_2$ can only be used for post-combustion capture technologies with a turnover T_2=600 K because its turnover temperature (T_1) is very high, outside

the temperature range of interest for pre-combustion applications.

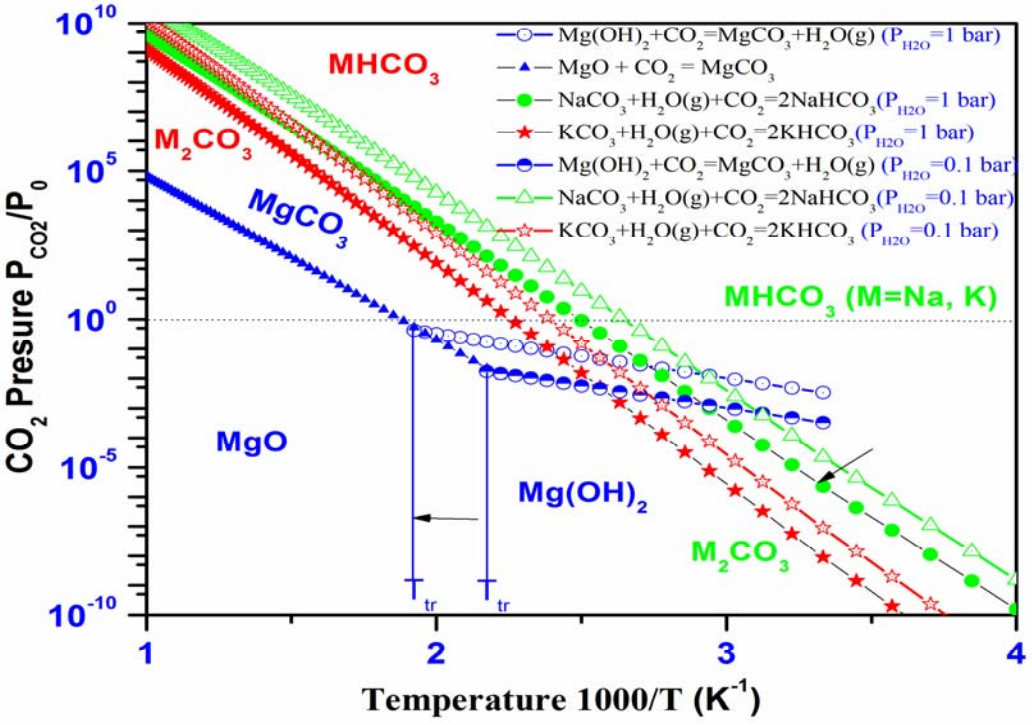

Figure 5. The calculated chemical potentials ($\Delta\mu$) versus CO_2 pressure P_{CO2}/P_0 and temperatures for the reactions of MgO, $Mg(OH)_2$, and alkali metal carbonates capturing CO_2 at fixed P_{H2O}= 1.0 bar and 0.1 bar.[18-19] Only the curve with $\Delta\mu$=0 for each reaction is shown explicitly.

Among these alkaline-earth metal oxides and hydroxides, comparing with CaO, only MgO and $Mg(OH)_2$ are found to be good sorbents for CO_2 capture. Upon absorption of CO_2 both of MgO and $Mg(OH)_2$ can form $MgCO_3$. However, the regeneration conditions of the original systems can take place at different conditions as indicated in Fig. 5. In this case we present the calculated phase diagram of MgO-$Mg(OH)_2$-$MgCO_3$ system at different CO_2 pressures and at two fixed P_{H_2O} values (0.1 and 1.0 bar). From Fig.5 it can be seen that when H_2O is present and at low temperatures, $MgCO_3$ can release CO_2 to form $Mg(OH)_2$ instead of forming MgO. For example, at P_{H_2O}=0.1 bar, only for temperatures under the transition temperature (T_{tr}) 460 K, $MgCO_3$ can be regenerated to form $Mg(OH)_2$. By the increase in the H_2O pressure, the transition temperature is increased. As shown in Fig.5, when P_{H_2O} is increased to 1.0 bar from 0.1 bar, the corresponding T_{tr} = 520K. Above T_{tr}, $MgCO_3$ is regenerated to MgO. Therefore, when water is present in the sorption/desorption cycle, no matter whether the initial sorbent is MgO or $Mg(OH)_2$, and for temperatures below T_{tr}, the CO_2 capture reaction is dominated by the process $Mg(OH)_2+CO_2 \leftrightarrow MgCO_3+ H_2O(g)$, whereas above T_{tr}, the CO_2 capture reaction is given by $MgO+CO_2 \leftrightarrow MgCO_3$. The reason is that between MgO and $Mg(OH)_2$, there is a phase transition reaction $MgO+H_2O(g)= Mg(OH)_2$ happening at the transition temperature T_{tr}. Obviously, by controlling the H_2O pressure as shown in Fig.5, the CO_2 capture temperature (T swing) can be adjusted because the CO_2 is a reactant while H_2O is a product. However, adding more water in the sorbent system will require more energy due to its sensible heat. These results are in good

agreement with the experimental measurements.[13]

3.2 Application to dehydrated and anhydrous potassium carbonates [15,22-23]

Hirano *et al.*[38] and Hayashi *et al.*[39] reported that the formation of active species, $K_2CO_3 \cdot 1.5H_2O$, plays an important role in the CO_2 capture capacity and that a vapor pretreatment process substantially improved CO_2 capture capacity.[40] The experimental results showed that the CO_2 capture capacity could be enhanced due to the conversion of the K_2CO_3 phase to the $K_2CO_3 \cdot 1.5H_2O$ phase through the $K_4H_2(CO_3)_3 \cdot 1.5H_2O$ phase during pretreatment with sufficient water vapor. [40] Shigemoto and Yanagihara[41] proposed potassium carbonate supported on an activated carbon as an efficient sorbent to recover CO_2 from moist flue gas through the reaction $K_2CO_3 \cdot 1.5H_2O + CO_2 = 2KHCO_3 + 0.5H_2O$. However, by using thermogravimetric analysis (TGA) and X-ray diffraction (XRD) measurements to obtain the characteristics of potassium-based sorbents for CO_2 capture, Zhao *et al.*[42] found that the carbonation reactivity of $K_2CO_3 \cdot 1.5H_2O$ and K_2CO_3 (in monoclinic structure and dehydrated from $K_2CO_3 \cdot 1.5H_2O$) was weak, but K_2CO_3 (in hexagonal structure) calcined from $KHCO_3$ showed excellent carbonation capacity and reproducibility. In order to evaluate the CO_2 capture performance of $K_2CO_3 \cdot 1.5H_2O$ and to compare with the corresponding anhydrous K_2CO_3, we will calculate the thermodynamic properties of CO_2 capture reactions by $K_2CO_3 \cdot 1.5H_2O$ and K_2CO_3 to find the optimal working conditions for achieving maximum capture capacity.

According to Eq.(3), the calculated heats of reaction (enthalpy change) for these two reactions versus temperature are plotted in Fig.6(a). Obviously, along the temperature range, the anhydrous K_2CO_3 capture of CO_2 can release more reaction heat than the hydrated $K_2CO_3 \cdot 1.5H_2O$. This means the interaction of K_2CO_3 with CO_2 is much stronger than that of $K_2CO_3 \cdot 1.5H_2O$, and during the regeneration stage, more energy is required to regenerate K_2CO_3. With P_{gas}=1 bar, Fig.6(b) shows the calculated Gibbs free energy of these two reactions versus temperature. The slope of the free energy versus temperature for reaction $K_2CO_3 + H_2O(g) + CO_2 = 2KHCO_3$ is larger than that of $K_2CO_3 \cdot 1.5H_2O + CO_2 = 2KHCO_3 + 0.5H_2O(g)$. This indicates that the driving force for $K_2CO_3 \cdot$ to capture a CO_2 is larger than that of $K_2CO_3 \cdot 1.5H_2O$, and the energy ($\Delta G>0$) needed to reverse the reaction $K_2CO_3 + H_2O(g) + CO_2 = 2KHCO_3$ is larger than that the reaction $K_2CO_3 \cdot 1.5H_2O + CO_2 = 2KHCO_3 + 0.5H_2O(g)$.

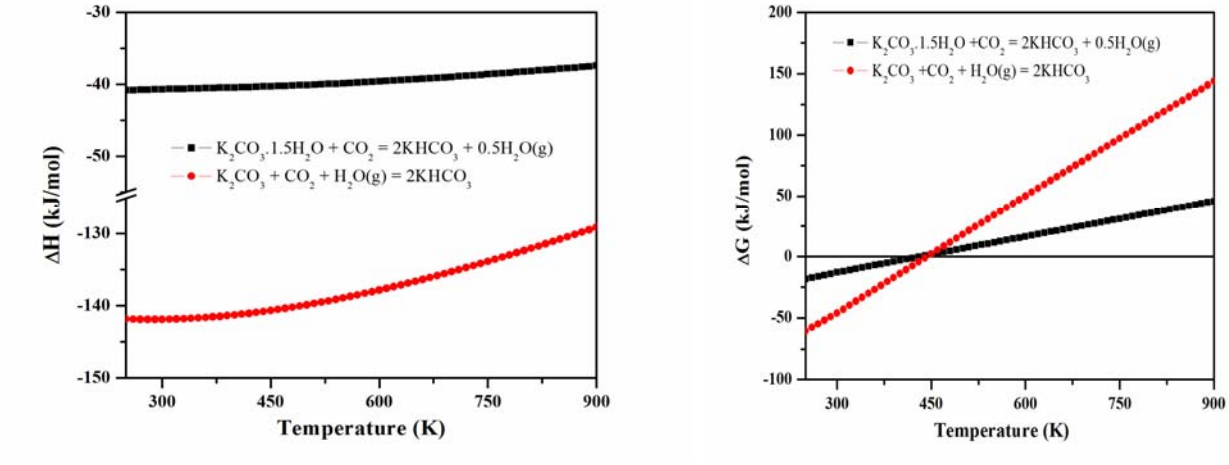

(a) (b)

Figure 6. The calculated thermodynamic properties of $K_2CO_3 \cdot 1.5H_2O$ and $K_2CO_3 \cdot$ reacting with CO_2. (a) Heat of reaction versus temperature; (b) Gibbs free energy versus temperature.[22]

By examining Eq.(2), for the reactions of $K_2CO_3 \cdot 1.5H_2O$ capturing CO_2, we can explore the relationship among chemical potential ($\Delta\mu(T,P)$), temperature, and CO_2 pressure (P_{CO_2}) at several fixed P_{H_2O}. This kind of relationship for these two reactions is shown in Fig.7 as a contour plot in a two dimensional representation. The lines in Fig.7 indicate conditions at which the $\Delta\mu(T,P)$ is zero. Near to these lines is a good region for energy efficient absorption and desorption because of the minimal energy costs at the given temperature and pressure. Above these lines in Fig.7 ($\Delta\mu(T,P)<0$), the solids $K_2CO_3 \cdot 1.5H_2O$ and K_2CO_3 are respectively favored to absorb CO_2 and to form $KHCO_3$, while below these lines ($\Delta\mu(T,P)<0$) the $KHCO_3$ is favored to release CO_2 regenerating the solid sorbent.

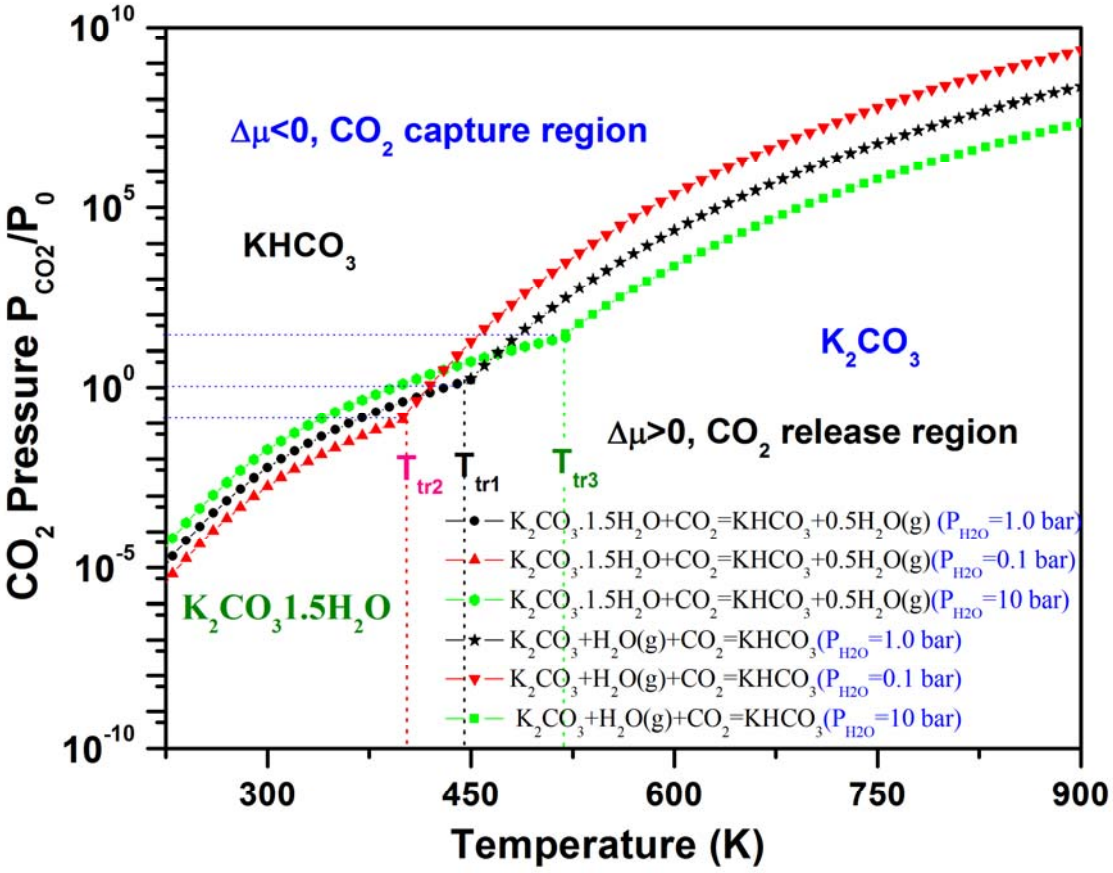

Figure 7. The contour plots of the calculated chemical potentials ($\Delta\mu$) versus temperatures and CO_2 pressures at several fixed H_2O pressures and temperatures for $K_2CO_3 \cdot 1.5H_2O$ and K_2CO_3 [15,19,22-23] capturing CO_2. Y-axis is given in logarithmic scale. Only $\Delta\mu=0$ curves with different fixed P_{H_2O} are shown explicitly. For each reaction, above the $\Delta\mu=0$ curve, the carbonates absorb CO_2 and the reaction goes forward ($\Delta\mu<0$ region) to form bicarbonate, whereas below the $\Delta\mu=0$ curve, the bicarbonate release CO_2 and the reaction goes backward to regenerate the carbonates ($\Delta\mu>0$ region).

From Fig.7 one can see that at each fixed P_{H_2O} these two lines of the reactions for $K_2CO_3 \cdot 1.5H_2O$ and $K_2CO_3 \cdot 1.5H_2O$ capturing CO_2 cross at a transition temperature (T_{tr}), which means

that at this temperature there is a phase transition $K_2CO_3 \cdot 1.5H_2O \leftrightarrow K_2CO_3 + 1.5H_2O$ happening. Obviously, at each fixed P_{H_2O}, the T_{tr} is fixed and does not depend on P_{CO_2} as shown with vertical line in Fig.7. Therefore, in Fig.7 the phase-diagram has three regions corresponding to three solid phases: the region below T_{tr} and under the line is $K_2CO_3 \cdot 1.5H_2O$, the region above T_{tr} and under the line is K_2CO_3, while the rest region above the lines is the $KHCO_3$ phase. In other words, below T_{tr} only $K_2CO_3 \cdot 1.5H_2O$ could be regenerated, while above T_{tr} the anhydrous K_2CO_3 could be regenerated. Table 1 summarizes the obtained results.

Table 1. The calculated thermodynamic properties of reactions of CO_2 captured by hydrated and dehydrated potassium carbonates in the unit of kJ/mol.[22] The highest temperature for carbonates capturing CO_2 at pre-combustion (T_1) (P_{CO2}=20 bar) and post-combustion (T_2) (P_{CO2}=0.1 bar) conditions as well as the phase transition temperature (T_{tr}) of $K_2CO_3 \cdot 1.5H_2O$ into K_2CO_3 are also given in this Table.

Reactions	CO_2 wt%	ΔE_{DFT}	ΔE_{ZP}	ΔH (T=300K)	ΔG (T=300K)	T_1 (K)	T_2 (K)	T_{tr} (K)
$K_2CO_3 \cdot 1.5H_2O + CO_2 = 2KHCO_3 + 0.5H_2O(g)$	26.88	-40.474	-0.737	-40.678	-12.820	580[b] 665[c] 510[d]	370[b] 395[c] 335[d]	445[b] 395[c] 515[d]
$K_2CO_3 + CO_2 + H_2O(g) = 2KHCO_3$	31.84	-154.429	18.293	-141.728 -142.854[a]	-46.281 -44.716[a]	490[b] 455[c] 515[d]	420[b] 395[c] 445[d]	

[a] Calculated by HSC Chemistry package[35]
[b] when P_{H_2O} = 1 bar
[c] when P_{H_2O} = 0.1 bar
[d] when P_{H_2O} = 10 bar

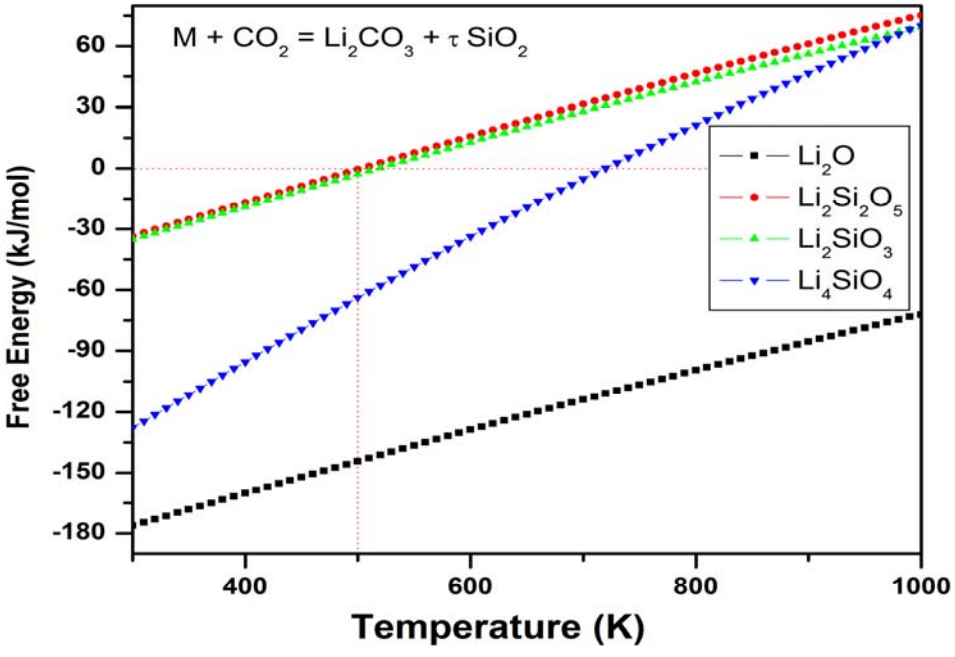

Figure 8. The Gibbs free energy changes of some lithium silicates capture CO_2 reactions from HSC Chemistry database.[35]

3.3 Applications to mixture of solids[14-16,20]

Lithium silicate (Li_4SiO_4) and zirconate (Li_2ZrO_3) have been proposed experimentally as promising high-temperature CO_2 sorbents.[43-49] And our previous theoretical studies confirmed these findings.[14-16] Figure 8 shows the free energy changes of CO_2 capture reactions by some lithium silicates as obtained from HSC Chemistry database. From Fig. 8, one can see that comparing with Li_2O, Li_4SiO_4, and Li_2ZrO_3, the Li_2SiO_3, $Li_2Si_2O_5$, and $Li_2Si_2O_7$ are better CO_2 solid sorbent candidates because they require less free energy to reverse the CO_2 capture reactions and have lower regenerating temperatures. Our calculations show that although pure Li_2O can absorb CO_2 efficiently, it is not a good solid sorbent for CO_2 capture because the reverse reaction, corresponding to Li_2CO_3 releasing CO_2, can only occur at very low CO_2 pressure and/or at very high temperature.[17] SiO_2 does not interact with CO_2 at normal conditions. Therefore, it can be concluded that when a lithium silicate compound with the ratio of Li_2O/SiO_2 is less or equal to 1.0, it could have better CO_2 capture performance than Li_4SiO_4, because its regeneration can occur at low temperature and hence require less regeneration heat. Further calculations (steps 3 and 4) and analysis on these lithium silicates capture CO_2 properties are underway.

Figure 9(a) summarizes our calculated heats of reaction (ΔH) for an alkali metal silicate and three zirconates.[14-16] From Fig. 9(a), one can see that the K_2ZrO_3 capture of CO_2 has a larger ΔH than the other three solids. Li_4SiO_4 has a relative small ΔH while along a large temperature range the Li_2ZrO_3 and Na_2ZrO_3 have similar ΔH. Therefore, K_2ZrO_3 is not a good CO_2 sorbent candidate because it needs more heat to regenerate. Among these four solids, Li_4SiO_4 is the best choice. These results are in good agreement with available experimental measurements.[43-49]

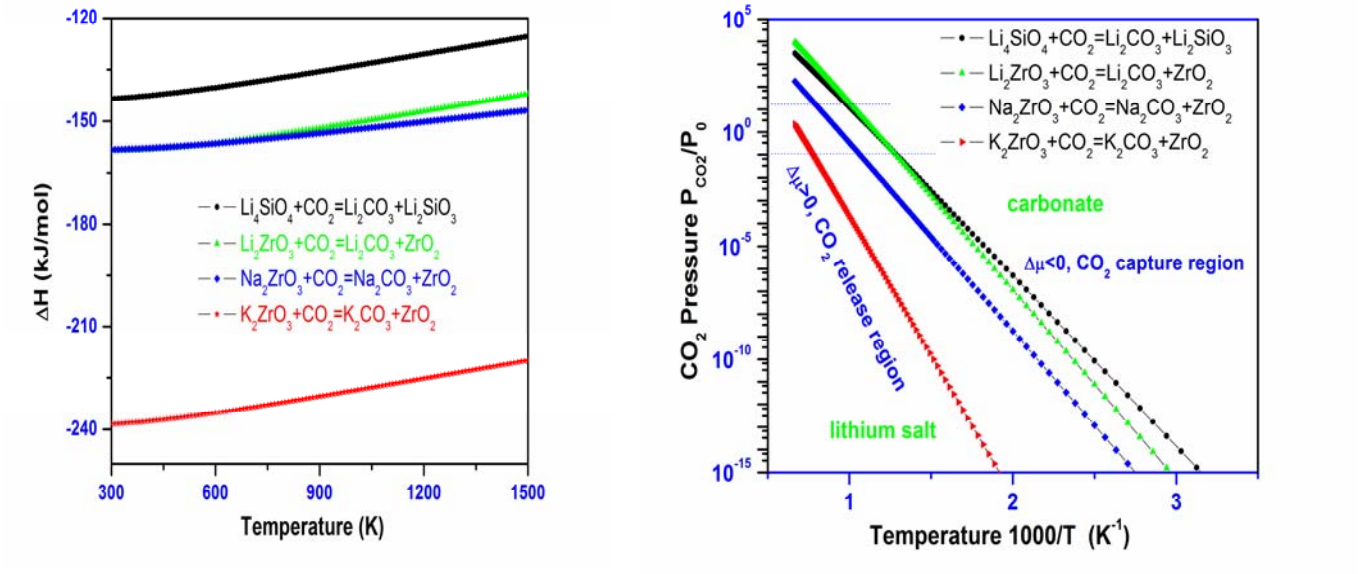

(a) **(b)**

Figure 9. The calculated thermodynamic properties of some alkali metal silicate and zirconates capture CO_2.[14-16] (a) The heat of reactions; (b) the contour plotting of calculated chemical potentials (Δμ) versus CO_2 pressures and temperatures of the sorbents capture CO_2 reactions. Y-axis plotted in logarithm scale. Only Δμ=0 curve is shown explicitly. For each reaction, above its Δμ=0 curve, their Δμ<0, which means the sorbents absorb CO_2 and the reaction goes forward, whereas below the Δμ=0 curve, their Δμ>0, which means the CO_2 start to release and the reaction goes backward to regenerate the sorbents.

According to Eq.(2), the calculated relationships of $\Delta\mu$ with CO_2 pressure and temperature for these four solids are shown in Fig.9(b). The line in Fig.9(b) indicates that for each reaction, $\Delta\mu(T, P)$ is approaching zero. The region close to the line is favorable for the absorption and desorption because of the minimal energy costs at a given temperature and pressure. Above the line, the solid (Li_4SiO_4, M_2ZrO_3 (M=Li, Na, K)) is favorable to absorb CO_2 and to form Li_2CO_3, while below the line the Li_2CO_3 is favorable to release CO_2 and to regenerate to lithium silicate solids. The calculated thermodynamic properties of these solids are also summarized in Table 2.

Table 2. The summary of the calculated energy change ΔE^{DFT}, the zero-point energy changes ΔE_{ZP} and the thermodynamic properties (ΔH, ΔG) of the CO_2 capture reactions by alkali metal silicates and zirconates. (unit: kJ/mol).[14-16,18] The turnover temperatures (T_1 and T_2) of the reactions of CO_2 capture by solids under the conditions of pre-combustion (P_{CO2}=20 bar) and post-combustion (P_{CO2}=0.1 bar) are also listed.

Reaction	ΔE^{DFT}	ΔE_{ZP}	ΔH (T=300K)	ΔG (T=300K)	Turnover T (K)	
					T_1	T_2
$Li_4SiO_4 + CO_2 \leftrightarrow Li_2CO_3 + Li_2SiO_3$	-148.704	5.971	-143.548	-93.972	1010	770
$Li_2ZrO_3 + CO_2 \leftrightarrow Li_2CO_3 + ZrO_2$	-146.648	11.311	-158.562 -162.69[a]	-103.845 -113.18[a]	1000	780
$K_2ZrO_3 + CO_2 \leftrightarrow K_2CO_3 + ZrO_2$	-223.158	5.813	-238.490	-187.884	hT[b]	1285
$Na_2ZrO_3 + CO_2 \leftrightarrow Na_2CO_3 + ZrO_2$	-140.862	2.236	-158.327 -151.403[a]	-114.121 -105.252[a]	1275	925

[a] from HSC-Chemistry database package[16]
[b] hT means the temperature is higher than our temperature range (1500 K)

From Fig.9(b) and Table 2 one can see that these solids capture CO_2 up to higher temperatures (T_1>1000K) compared with the desired pre-combustion condition (313~573K). Therefore, they are not good sorbents for capturing CO_2 in pre-combustion technology. However, some of them could be used for high-temperature post-combustion CO_2 capture technology with T_2=1285K, 925 K, 780K, and 770K for K_2ZrO_3, Na_2ZrO_3, Li_2ZrO_3 and Li_4SiO_4 respectively. Obviously, compared to CaO, the T_2 of K_2ZrO_3 is still too high to be used for post-combustion technology. This may be part of the reason that there is no experimental work found in the literature for pure K_2ZrO_3 capturing CO_2. Therefore, Li_4SiO_4, Na_2ZrO_3, and Li_2ZrO_3 are good candidates for CO_2 sorbents working at high temperature.

Although Li_4SiO_4 and Li_2ZrO_3 have similar turnover temperature T_2 as shown in Table 2, from Fig.9(a) one can see that the reaction heat of Li_2ZrO_3 capture of CO_2 is about 20 kJ/mol lower than that of Li_4SiO_4. This indicates that more heat is needed for regenerating Li_2ZrO_3 from Li_2CO_3 and ZrO_2. Therefore, as a CO_2 sorbent, the Li_4SiO_4 is thermodynamically better than Li_2ZrO_3, despite they may have different kinetics behaviors.[50]

4 Conclusions

By combining thermodynamic database searching with first principles density functional theory and phonon lattice dynamics calculations, with a vast array of solid materials, we proposed a

theoretical screening methodology to identify promising candidates for CO_2 sorbents. The thermodynamic properties of solid materials are obtained and used for computing the thermodynamic reaction equilibrium properties of CO_2 absorption/desorption cycle based on the chemical potential and heat of reaction analysis. According to the pre- and post-combustion technologies and conditions in power-plants, based on our calculated thermodynamic properties of reactions for each solid capturing CO_2, only those solid materials, which result in lower energy cost in the capture and regeneration process and could work at desired conditions of CO_2 pressure and temperature, will be selected as CO_2 sorbent candidates and further be considered for experimental validation. Compared to experimental thermodynamic data for known systems, our results show that this screening methodology can predict the thermodynamic properties for CO_2 capture sorbents reactions and therefore can be used for screening from vast numbers of solid materials where thermodynamic data are unknown.

Acknowledgement

The author thanks Drs. D. C. Sorescu, D. Luebke, H. Pennline, J. K. Johnson, B. Zhang, Y. Soong, R. Siriwardane, J. W. Halley and G. Richards for fruitful discussions.

References

(1) Aaron, D.; Tsouris, C. *Separation Science and Technology* **2005**, *40*, 321.
(2) Allen, M. R.; Frame, D. J.; Huntingford, C.; Jones, C. D.; Lowe, J. A.; Meinshausen, M.; Meinshausen, N. *Nature* **2009**, *458*, 1163.
(3) Haszeldine, R. S. *Science* **2009**, *325*, 1647.
(4) MacDowell, N.; Florin, N.; Buchard, A.; Hallett, J.; Galindo, A.; Jackson, G.; Adjiman, C. S.; Williams, C. K.; Shah, N.; Fennell, P. *Energy & Environmental Science* **2010**, *3*, 1645.
(5) Markewitz, P.; Kuckshinrichs, W.; Leitner, W.; Linssen, J.; Zapp, P.; Bongartz, R.; Schreiber, A.; Muller, T. E. *Energy & Environmental Science* **2012**, *5*, 7281.
(6) White, C. M.; Strazisar, B. R.; Granite, E. J.; Hoffman, J. S.; Pennline, H. W. *Journal of the Air & Waste Management Association* **2003**, *53*, 645.
(7) Figueroa, J. D.; Fout, T.; Plasynski, S.; McIlvried, H.; Srivastava, R. D. *International Journal of Greenhouse Gas Control* **2008**, *2*, 9.
(8) Rubin, E. S.; Mantripragada, H.; Marks, A.; Versteeg, P.; Kitchin, J. *Progress in Energy and Combustion Science* **2012**, *38*, 630.
(9) Duan, Y. *Proceedings of 7th~10th Annual Conference on Carbon Capture and Sequestration* **2008-2011**.
(10) White, C. M.; Strazisar, B. R.; Granite, E. J.; Hoffman, J. S.; Pennline, H. W. *J Air Waste Manag Assoc* **2003**, *53*, 645.
(11) Abanades, J. C.; Anthony, E. J.; Wang, J.; Oakey, J. E. *Environ. Sci. Technol.* **2005**, *39*, 2861.
(12) Siriwardane, R.; Poston, J.; Chaudhari, K.; Zinn, A.; Simonyi, T.; Robinson, C. *Energy & Fuels* **2007**, *21*, 1582.
(13) Siriwardane, R. V.; Stevens, R. W. *Industrial & Engineering Chemistry Research* **2009**, *48*, 2135.
(14) Duan, Y. *Journal of Renewable and Sustainable Energy* **2011**, *3*, 013102.
(15) Duan, Y. *Journal of Renewable and Sustainable Energy* **2012**, *4*, 013109.
(16) Duan, Y.; Parlinski, K. *Physical Review B* **2011**, *84*, 104113.
(17) Duan, Y.; Sorescu, D. C. *Physical Review B* **2009**, *79*, 014301.
(18) Duan, Y.; Sorescu, D. C. *Journal of Chemical Physics* **2010**, *133*, 074508.
(19) Duan, Y.; Zhang, B.; Sorescu, D. C.; Johnson, J. K. *J. Solid State Chem.* **2011**, *184*, 304.
(20) Zhang, B.; Duan, Y.; Johnson, J. K. *Journal of Chemical Physics* **2012**, *136*, 064516.

(21) Duan, Y.; Luebke, D.; Pennline, H. *International Journal of Clean Coal and Energy* **2012**, *1*, 1.
(22) Duan, Y. H.; Luebke, D. R.; Pennline, H. W.; Li, B. Y.; Janik, M. J.; Halley, J. W. *Journal of Physical Chemistry C* **2012**, *116*, 14461.
(23) Duan, Y. H.; Zhang, B.; Sorescu, D. C.; Johnson, J. K.; Majzoub, E. H.; Luebke, D. R. *Journal of Physics-Condensed Matter* **2012**, *24*.
(24) Kresse, G.; Hafner, J. *Phys. Rev. B* **1993**, *47*, 558.
(25) Kresse, G.; Furthmuller, J. *Phys. Rev. B* **1996**, *54*, 11169.
(26) Perdew, J. P.; Wang, Y. *Physical Review B* **1992**, *45*, 13244.
(27) Duan, Y. *Phys. Rev. B* **2008**, *77*, 045332.
(28) Monkhorst, H. J.; Pack, J. D. *Phys. Rev. B* **1976**, *13*, 5188.
(29) Parlinski, K. *Software PHONON* **2006**.
(30) Parlinski, K.; Li, Z. Q.; Kawazoe, Y. *Phys. Rev. Lett.* **1997**, *78*, 4063.
(31) Sternik, M.; Parlinski, K. *J. Chem. Phys.* **2005**, *123*.
(32) *DOE-NETL : "Cost and Performance Baseline for Fossil Energy Plants", Volume 1: Bituminous Coal and Natural Gas to Electricty Final Report*; http://www.netl.doe.gov/energy-analyses/baseline_studies.html, 2007.
(33) Mathias, P. M.; Reddy, S.; O'Connell, J. P. *International Journal of Greenhouse Gas Control* **2010**, *4*, 174.
(34) Wang, Q.; Luo, J.; Zhong, Z.; Borgna, A. *Energy & Environmental Science* **2011**, *4*, 42.
(35) *HSC Chemistry software 6.1, Pori: Outotec Research Oy, www.outotec.com/hsc* **2006**.
(36) Factsage. www.factsage.com, 2006-2010.
(37) Pennline, H. W.; Hoffman, J. S.; Gray, M. L.; Siriwardane, R. V.; Fauth, D. J.; Richards, G. A. NETL in-house postcombustion sorbent-based carbon dioxide capture research. In *Annual NETL CO2 capture technology for existing plants R&D meeting* Pittsburgh, 2009.
(38) Hirano, S.; Shigemoto, N.; Yamada, S.; Hayashi, H. *Bull. Chem. Soc. Jpn.* **1995**, *68*, 1030.
(39) Hayashi, H.; Taniuchi, J.; Furuyashiki, N.; Sugiyama, S.; Hirano, S.; Shigemoto, N.; Nonaka, T. *Ind. Eng. Chem. Res.* **1998**, *37*, 185.
(40) Lee, S. C.; Kim, J. C. *Catal Surv Asia* **2007**, *11*, 171.
(41) Shigemoto, N.; Yanagihara, T.; Sugiyama, S.; Hayashi, H. *Energy Fuels* **2006**, *20*, 721.
(42) Zhao, C. W.; Chen, X. P.; Zhao, C. S.; Liu, Y. K. *Energy Fuels* **2009**, *23*, 1766.
(43) Essaki, K.; Nakagawa, K.; Kato, M.; Uemoto, H. *J. Chem. Eng. Jpn* **2004**, *37*, 772.
(44) Kato, M.; Nakagawa, K. *J. Ceram. Soc. Jpn* **2001**, *109*, 911.
(45) Nakagawa, K.; Ohashi, T. *J. Electrochem. Soc.* **1998**, *145*, 1344.
(46) Nakagawa, K.; Ohashi, T. *Electrochemistry* **1999**, *67*, 618.
(47) Olivares-Marin, M.; Drage, T. C.; Maroto-Valer, M. M. *International Journal of Greenhouse Gas Control* **2010**, *4*, 623.
(48) Rodriguez-Mosqueda, R.; Pfeiffer, H. *Journal of Physical Chemistry A* **2010**, *114*, 4535.
(49) Xiong, R.; Ida, J.; Lin, Y. S. *Chemical Engineering Science* **2003**, *58*, 4377.
(50) Lopez-Ortiz, A.; Rivera, N. G. P.; Rojas, A. R.; Gutierrez, D. L. *Separation Science and Technology* **2004**, *39*, 3559.